Annu. Rev. Biophys. Biomol. Struct. 2003. 32:183–206
doi: 10.1146/annurev.biophys.32.110601.141906

First published online as a Review in Advance on February 5, 2003

THE STRUCTURE OF MAMMALIAN CYCLOOXYGENASES

R. Michael Garavito and Anne M. Mulichak
Department of Biochemistry and Molecular Biology, Michigan State University, East Lansing, Michigan 48824-1319; email: garavito@msu.edu; mulichak@msu.edu

Key Words prostaglandin H_2 synthase, heme-dependent peroxidase, arachidonic acid, nonsteroidal antiinflammatory drugs, COX-2-selective inhibitors

■ **Abstract** Cyclooxygenases-1 and -2 (COX-1 and COX-2, also known as prostaglandin H_2 synthases-1 and -2) catalyze the committed step in prostaglandin synthesis. COX-1 and -2 are of particular interest because they are the major targets of nonsteroidal antiinflammatory drugs (NSAIDs) including aspirin, ibuprofen, and the new COX-2-selective inhibitors. Inhibition of the COXs with NSAIDs acutely reduces inflammation, pain, and fever, and long-term use of these drugs reduces the incidence of fatal thrombotic events, as well as the development of colon cancer and Alzheimer's disease. In this review, we examine how the structures of COXs relate mechanistically to cyclooxygenase and peroxidase catalysis and how alternative fatty acid substrates bind within the COX active site. We further examine how NSAIDs interact with COXs and how differences in the structure of COX-2 result in enhanced selectivity toward COX-2 inhibitors.

CONTENTS

CYCLOOXYGENASE

The cyclooxygenases (COXs), which are also known as prostaglandin H_2 synthases (EC 1.14.99.1), are bifunctional, membrane-bound enzymes that catalyze the committed step in prostanoid biosynthesis (45, 74, 76). Prostanoids are members of a large group of bioactive, oxygenated C_{18}–C_{22} compounds that are derived from ω3 (n-3) and ω6 (n-6) polyunsaturated fatty acids. In mammals, arachidonic acid (AA; 20:4 n-6) is the major prostanoid precursor. The heme-dependent bis-oxygenase or COX reaction converts AA to PGG_2, a 9,11-endoperoxide-15-hydroperoxide product (Figure 1). The subsequent peroxidase (POX) reaction reduces the 15-hydroperoxide of PGG_2 to form PGH_2.

The COX reaction also is the target of aspirin, ibuprofen, and other nonsteroidal antiinflammatory drugs (NSAIDs), which account for billion of dollars in sales for the pharmaceutical industry. By the end of the 1980s, the interaction of aspirin and other NSAIDs with COX had been well studied, and many felt that this area of pharmacological research had played out. However, the discovery that two isoforms of COX exist in mammals radically changed our understanding of prostanoid physiology and NSAID pharmacology (20, 76) and triggered a phenomenal increase in interest in the structure, function, and physiology of COXs during the late 1990s. Moreover, an increasing amount of evidence suggested that the COX isozymes have direct roles in many human pathologies. These include thrombosis (55, 56), inflammation, pain and fever (5), various cancers (21, 48, 82),

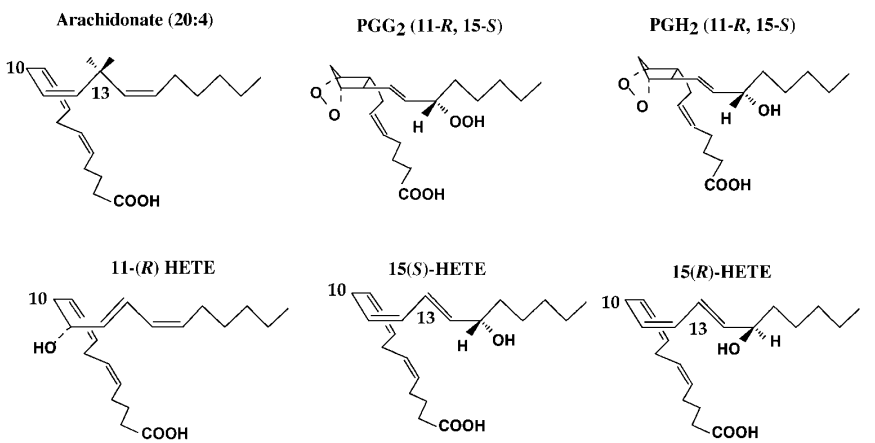

Figure 1 Schematic diagrams of arachidonic acid and the oxygenated products produced by COX-1 and -2. PGG_2, the primary product of the native enzymes, is reduced to PGH_2 at the POX active site of the COXs. 11*R*-hydroxy-(5Z,8Z,12E,13Z)-eicosatetraenoic acid (11*R*-HETE) and 15-hydroxy-(5Z,8Z,11Z,13E)-eicosatetraenoic acid (15*R*-HETE and 15*S*-HETE) are the minor products found after the reduction of their respective hydroperoxy precursors (see text).

and neurological disorders such as Alzheimer's (46) and Parkinson's (79) diseases. Finally, pharmacological research over the past decade led to the development and approval of the new COX-2-selective NSAIDs (e.g., Celebrex® and Vioxx®), which target COX-2 instead of COX-1. Armed with a panoply of new and classical COX inhibitors, researchers have begun to discover NSAID-dependent physiological effects that are seemingly not directly related to COX inhibition and the subsequent cessation of prostanoid biosynthesis. These COX-independent phenomena include the antitumor activities of some NSAIDs (63, 82), and the effects of aspirin on beta-amyloid formation in Alzheimer's disease (84) have provoked a new series of controversies about the physiological roles of the COX isozymes and the pharmacological actions of NSAIDs.

Although research on COXs has resulted in a vast amount of information about the molecular biology, pharmacology, and structural biology of these enzymes, new mysteries about the biochemistry and enzymology of the COX isoforms have arisen. The reader is encouraged to read a number of recent reviews on the physiology, enzymology, and pharmacology of these enzymes (12, 29, 43, 45, 76). In this review, we discuss the structures of the COX isoforms and their relevance to their function.

THE COX REACTION

Ruf and coworkers (9) first proposed a branched-chain, mechanistic model (Figure 2) that incorporates the requirement of heme oxidation by the COX reaction. In this scheme, a hydroperoxide reacts with the heme iron to initiate a two-electron oxidation that yields Compound I, an enzyme state with an oxyferryl-heme radical cation. Compound I quickly undergoes a single electron reduction via an intramolecular migration of the radical from the heme group to Tyr385 to create Intermediate II (77, 88). When the COX active site is occupied by an appropriate fatty acid substrate such as AA, the tyrosyl radical initiates the COX reaction by abstracting the 13*proS* hydrogen to yield an arachidonyl radical (88). The fatty acid radical then reacts with molecular O_2 to produce an 11-hydroperoxyl radical, which in turn forms the endoperoxide cyclopentane moiety of PGH_2; the addition of a second O_2 molecule at carbon 15 ultimately produces PGG_2.

The POX reaction then comes into play again to reduce the 15-hydroperoxide of PGG_2 to form PGH_2. Although the POX reaction is considered the second step in the formation of PGH_2, the COX reaction is absolutely dependent on POX activity for its activation (77, 76). Initially, the ambient hydroperoxides activate the COX reaction in a small number of COX molecules via POX turnovers. As more PGG_2 is generated, the remaining COX molecules are then activated autocatalytically. In vitro this phenomenon is exhibited as the lag period seen in COX activity assays (27).

While COX-1 synthesizes primarily PGG_2 from AA, it also produces small but significant amounts of other products (67, 85, 86) (Figure 1): 11*R*-hydroperoxy-(5Z,8Z,12E,13Z)-eicosatetraenoic acid (11*R*-HPETE) and

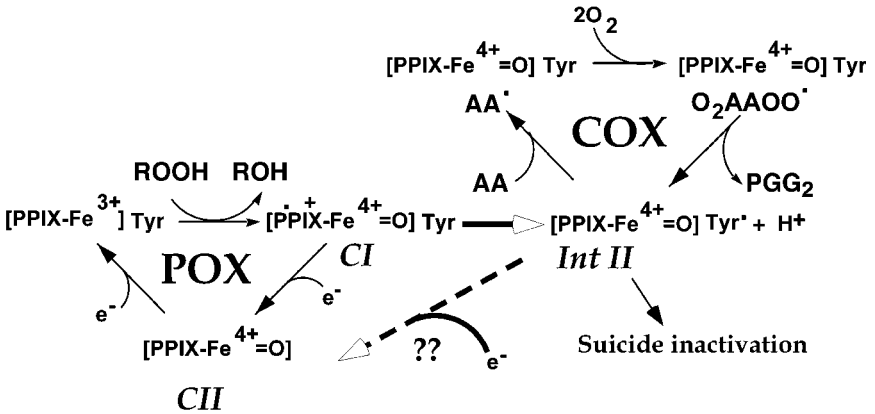

Figure 2 A schematic diagram of the branched-chain reaction mechanism for the COX enzymes that was originally proposed by Ruf and colleagues (9). In essence, one turnover of the POX reaction is needed to provide the tyrosyl radical for activating the COX reactions. Activated COX would continue to turnover, in the presence of substrate, until radical induced inactivation occurs (77, 76). The diagram was adapted from Reference 76.

15-hydroperoxy-(5Z,8Z,11Z,13E)-eicosatetraenoic acid (15*R*-HPETE and 15*S*-HPETE). The kinetics of the product formation suggests that AA may adopt up to four slightly different but catalytically competent conformers in the COX active site that then give rise to the different oxygenated products (86). Human COX-2 was also thought to form only PGG_2, 11*R*-HPETE, and 15*S*-HPETE but not 15*R*-HPETE (94), which suggested that there are only three catalytically competent conformers of AA in this isoform. However, more recent work by Schneider et al. (67) shows that wild-type COX-2 does form 15*R*-HPETE.

COX-1 and -2 also catalyze the oxygenation of other polyunsaturated fatty acids into bioactive compounds (23, 24, 40, 62, 70, 87). Both COX-1 and -2 produce the series-1 prostaglandin precursor PGH_1 from dihomo-γ-linolenic acid (DHLA; 20:3n-6) and the series-3 prostaglandin precursor PGH_3 from eicosapentaenoic acid (EPA, 20:5n-3), a dietary ω-3 fatty acid that has been linked to reduced cardiovascular disease (70). Linolenic acid (LA; 18:2n-6) is converted to 9- and 13-hydroxyoctadecadienoic acids (40). The ability of the COX enzymes to use alternative substrates demonstrates the impact of diet on physiology.

GENERAL ASPECTS OF COX STRUCTURE

After the discovery of the COX isoforms, it quickly became apparent that the isoforms were noticeably different in their expression profiles and roles in several physiological processes (20, 76). COX-1 is the constitutively expressed isoform

and is apparently involved in many aspects of physiological homeostasis. On the other hand, COX-2 is the inducible isoform whose expression in a select number of cells is triggered by specific cellular events. However, both enzymes are membrane bound and are present on the lumenal surfaces of the endoplasmic reticulum and of the inner and outer membranes of the nuclear envelope (49, 83).

The primary structures of nascent COX-1 and -2 are 600–602 (depending on the species) and 604 amino acids, respectively (75), and both isoforms are then processed into mature forms by removal of signal peptides. The high degree of sequence identity between the processed isoforms and between species allows an almost one-to-one comparison (74, 76). By convention, the residues of COX are often numbered to correspond to the ovine or murine COX-1 sequence (75) to aid convenience of structural and functional comparisons across species. Sequence comparisons between COX isoforms from the same species show 60%–65% sequence identity, while sequence identity among orthologs from different species varies from 85% to 90% (75). When compared with sequences from other proteins, particularly other heme-dependent peroxidases, significant levels of similarity were detected. Clearly, the COX enzymes are members of the mammalian heme-dependent peroxidase family (61, 95), which includes myeloperoxidase (MPO) and thyroid peroxidase. Moreover, both isoforms contain an epidermal growth factor (EGF)-like domain just C-terminal to the signal peptide. The role of the EGF domain remains unclear, but it was noted that the EGF domains also occur in many cell surface membrane proteins (3).

Despite a high level of sequence homology between COX isoforms, major differences in primary structure occur in three distinct areas of the sequence. First, both isoforms have distinctly different signal peptides in terms of length and amino acid composition. Second, substantial sequence differences are found in the membrane binding domains (MBDs) between the two isoforms (54, 83), although no explanation for this phenomenon is known. Third, sequences of COX-2, but not COX-1, contain an insert of 18 amino acids that is six residues in from the C terminus. The function of this insert in COX-2 is not known, but mutations and sequence alterations at the C terminus can markedly affect the expression of active protein (17, 81). In contrast, N-terminal His-tagged versions of human COX-1 and -2 have been prepared and expressed in high yield in insect cell culture (73). In all cases, the addition of the N-terminal hexaHis-tag, between the signal peptide and the EGF domain, does not apparently impact the folding of the heterologously expressed enzyme or its activity.

Purified native COX-1 appears to be uniformly glycosylated at three sites (Asn68, Asn144, and Asn410) and appears as a single band on SDS-PAGE with a M_{app} ~67 KDa. Native COX-2, on the other hand, is more heterogeneously glycosylated at an additional site (Asn588), and multiple molecular species of COX-2 can be readily observed with SDS-PAGE with a M_{app} 68–72 KDa (53). N-glycosylation may play a role in the maturation of COXs (53), but the deglycosylation of the mature enzyme does not affect activity. Moreover, COX-1 and -2

appear as homodimers in solution after detergent solubilization (74, 76), whether glycosylated or not.

The COXs bind 1 mole of ferric-protoporphyrin IX per mole monomer for full activity, as expected for a heme-dependent peroxidase. However, native ovine COX-1 often loses much of the bound heme during detergent solubilization and purification (39, 91). For recombinant COX-2, detergent solubilization and subsequent purification tends to yield apo-enzyme (1, 14, 73), suggesting that its affinity for heme is lower than that exhibited by COX-1. Although the heme can be readily removed, active COX-1 and -2 can be easily reconstituted by the addition of hematin to the sample. This behavior makes the COXs rather unusual among the known heme-dependent peroxidases. Moreover, COXs can readily bind manganoprotoporphyrin IX or cobalt-protoporphyrin IX to create novel holo-species that are structurally native but have quite altered activity (39, 89, 90).

THE TERTIARY STRUCTURE OF THE COX ENZYMES

In 1994, Picot et al. (58) published the first three-dimensional structure of a COX enzyme, the ovine COX-1 complexed with the NSAID flurbiprofen (Figure 3*a*). Soon afterward, the crystal structures of human (37) and murine (28) COX-2 followed. Drug interactions with COX were one of the first issues to be addressed, and complexes containing a number of different NSAIDs have been studied crystallographically with COX-1 (34–36, 69) and COX-2 (28, 37). The structural analysis of COX complexed with substrates or products was more difficult to pursue for a number of technical reasons, particularly the sensitivity of polyunsaturated fatty acids to oxidation. However, within the past three years, structures of ovine COX-1 complexed with several different fatty acid substrates have been published: with AA (20:4n-6) (38), dihomo-γ-linolenic acid (DHLA; 20:3n-6) (87), linolenic acid (LA; 18:2n-6) (40), and eicosapentaenoic acid (EPA; 20:5n-3) (40). Likewise, crystal structures of murine COX-2 complexed with AA (22) and EPA (29) have also been determined.

As was expected from the observed levels of sequence identity, the crystal structures verified that the COX isoforms are structurally homologous and quite superimposable (28, 37). The COX monomer (Figure 3*b*) consists of three structural domains: the N-terminal EGF domain, a membrane binding domain (MBD) of about 48 amino acids in length, and a large C-terminal globular catalytic domain containing the heme binding site. The C-terminal segments beyond Pro583 (17 amino acids in COX-1 and 35 amino acids in COX-2) have not been resolved crystallographically (28, 37, 58).

Epidermal Growth Factor Domain

The EGF and catalytic domains create the subunit interface in the dimer and place the two MBDs in a homodimer about 25 Å apart (Figure 3*a*). The EGF domains create a substantial portion of the dimer interface. EGF domains are common in several families of membrane proteins and secreted proteins (3). Typically, the EGF

domain occurs at a position in the primary sequence N-terminal to a membrane anchor, such that these domains always occur on the extracytoplasmic face of the membrane. Garavito and colleagues (13, 57) have suggested that the EGF domains may play a role in the insertion of COX into the lipid bilayer.

Membrane Binding Domain

The MBD of COX is built up of four short consecutive amphipathic α-helices (Figure 3*b*); three of the four helices lie roughly in the same plane while the last helix angles "upward" into the catalytic domain. Hydrophobic and aromatic residues protrude from these helices to create a hydrophobic surface that would interact with only one face of the lipid bilayer (58). The MBD of COX-1 and -2 thus represents the first example of "monotopic" insertion into biological membranes. The physical and biological consequences of monotopic anchoring have been studied biochemically (33) and by computer modeling (51). The COX isozymes can only be isolated from the membrane using detergents (1, 14, 27), demonstrating that monotopic anchoring can create truly integral membrane proteins. Moreover, the COX isozymes were all crystallized in the presence of nonionic detergents, and tightly bound detergent molecules have been clearly resolved in the COX crystal structures (34, 35, 37, 38).

Catalytic Domain

The catalytic domain comprises the bulk of the COX monomer (13) and is almost entirely composed of α-helical secondary structure. The COX catalytic domain shares a great deal of structural homology with mammalian MPO (13, 58), consistent with the sequence comparisons. Structural homology between the COX catalytic domain and nonmammalian heme-dependent peroxidases is also detectable (13, 58, 61). The POX active site is in a large groove on the side opposite of the MBD (Figure 3*b*), while the entrance to the COX active site is between the helices of the MBD. The hydrophobic COX channel extends from the MBD into the interior of the catalytic domain (58), a distance of about 25 Å (Figure 3*c*). The COX channel contains several side pockets (28, 37, 58) as well as water channels (68) that extend from the COX active site near Gly533 to the dimer interface. At the interface between the MBD and catalytic domain, the COX channel narrows considerably to form an aperture that divides the COX channel into a mouth (or "foyer") and a catalytic center (Figure 3*c*). The narrowness of the aperture clearly suggests that the MBD may undergo significant conformational changes during entry of fatty acid substrates and NSAIDs (35).

THE EVOLUTION OF COX

How COX evolved from soluble heme-dependent peroxidases is an intriguing question and shows the ingenuity of Nature's biological engineering. Several crystal structures are currently available for heme-dependent peroxidases including

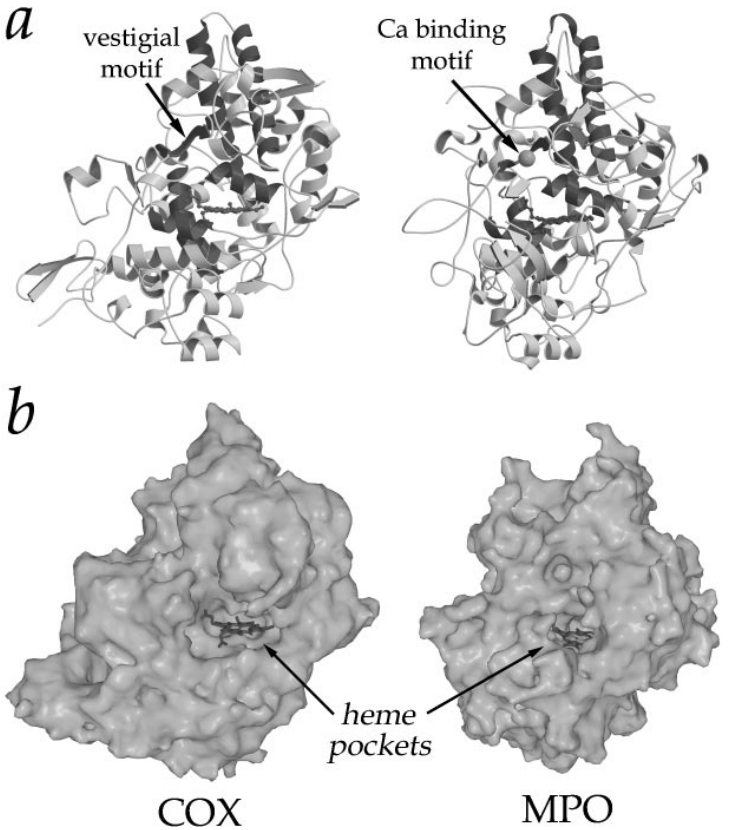

Figure 4 Views of POX active site of the COX-1 monomer with respect to myeloperoxidase (MPO) after superposition. (*a*) The structurally homologous helices that have catalytic relevance are in a *darker gray* (see text). The functioning and vestigial calcium binding motifs are *dark gray* in MPO and COX, respectively. (*b*) An accessible surface view of the POX active site shows how exposed the heme is to solvent compared to that in MPO. Molscript (25) and Raster3D (47) were used to draw (*a*).

mammalian myeloperoxidase (MPO) (6, 95), yeast cytochrome *c* peroxidase (60), and lignin peroxidase (59). Among these, MPO displays obvious close structural homology to the COX catalytic domain, with an rms deviation of 1.5 Å on C_α atoms after relative insertions/deletions are accounted for (Figure 4*a*). The most notable differences between the two enzymes are two long loops that are inserted in the MPO structure and serve to cover the heme binding pocket.

When COX is superimposed with the more distantly related nonmammalian peroxidases by aligning the proximal and distal His residues of the heme pocket, it is clear that the topologies are homologous, including a conserved spatial and

topological arrangement of six helices (Figure 4*a*). Using the MPO/COX helix nomenclature (95), these helices are *helix 2*, which bears the distal His residue; *helices 5* and *6*, arranged in a distinctive helix-turn-helix motif; *helix 8*, which carries the proximal histidine residue; *helix 12*, which packs against *helix 8* in an antiparallel manner; and the long *helix 17*, which forms part of the COX channel. Optimally superimposing the conserved helices of COX with the nonmammalian peroxidases yields rms deviations on C_α atoms around 3 to 4 Å.

In addition to the series of conserved helices, COX, MPO, and several nonmammalian peroxidases retain another structural feature: a calcium-binding motif that occurs adjacent to the heme pocket (Figure 4*a*) and after *helix 2* in the sequence. This motif consists of a tight turn of the main chain and is typically composed of a (Val-X-)Gly-X-Asp-X-Ser sequence. A carboxylate oxygen of the Asp in this motif forms hydrogen bonds that bridge the Gly carbonyl and Ser amide main chain groups. The cation is coordinated by the Val and Gly carbonyl groups and the Asp and Ser side chains, as well as both carbonyl and side chain oxygen atoms from an Asp residue immediately following the distal His. This motif is highly conserved in the plant and mammalian enzymes (61); however, in both fungal peroxidases, the interaction with the initial carbonyl group is absent (59). Despite the lack of cation binding, COX retains a vestigial G-X-D-X-G calcium-binding motif (Figure 4*a*), where a Gly is substituted for the usual Ser residue, with a conserved main chain conformation and the Asp side chain making analogous hydrogen bonds with the adjacent main chain. A vestigial G-X-D-X-G calcium-binding motif also exists in the structure of yeast cytochrome *c* peroxidase, which also does not bind calcium. These features clearly demonstrate the evolutionary relationship between fungal, plant, and mammalian peroxidases.

THE POX ACTIVE SITE

The POX active sites in the COXs are quite open to the solvent in contrast to virtually all other peroxidases (Figure 4*b*). As noted above, this gives rise to the rather facile manner by which the heme can be removed and then reconstituted. Within the heme pocket, the mammalian peroxidases COX and MPO also bind the heme ring in an orientation of bound heme that is rotated 180° relative to that seen in the nonmammalian peroxidases. This results in the propionate moieties extending in the opposite direction.

In the refined crystal structure of ovine COX-1 (68), the POX active site (Figure 5) reveals that His388 is the proximal heme ligand: The Nε nitrogen bonds to the ferric iron while the Nδ participates in a hydrogen bond network involving a water molecule and Tyr504. In COX-2, the identical arrangement is seen but the existence of a proximal water molecule has not been commented on (28, 37). In contrast, the proximal His forms a hydrogen bond with a conserved Asp side chain on an adjacent helix in the plant, yeast, and fungal peroxidases (11, 61); in MPO, the proximal His residue interacts instead with an Asn side chain (6). Thus, the proximal histidine in COX does not form an ionic

bond or strong hydrogen bond, which may make the proximal His more neutral (66, 68).

On the distal side of the heme (Figure 5), His207 is predicted to be important in the deprotonation of the peroxide substrate and subsequent reprotonation of the incipient alkyloxide ion to form the alcohol during generation of Compound I (30). In both COX and MPO, a conserved Gln side chain (Gln203 in COX and Gln91 in canine MPO) is also found adjacent to the distal His in place of the Arg residue usually found in nonmammalian peroxidases. The side chain of the distal His appears to be oriented by hydrogen bonding to the Gln main chain carbonyl, as well as to the side chain immediately preceding the His (Thr206 for COX, Asp94 for MPO). Moreover, orientation of the distal His is usually stabilized by hydrogen bonding to a highly conserved Asn side chain located across the heme binding pocket. Hence, the imidazole ring of the distal His is rotated 180° in COX and MPO relative to that found in the nonmammalian peroxidases. Mutations of Gln203, His207, or His388 in ovine COX-1 and human COX-2 lead to a reduction or elimination of POX activity (30, 71).

Typical heme iron ligands (e.g., CO or CN^-) bind to the distal side of the iron with a linear or "unbent" geometry in ovine COX-1 (68). This seems to be a reasonable result, as COX has a very open active site (Figure 4*b*) and must bind large ligands such as 15-HPETE or PGG_2. However, COX-1 paradoxically exhibits reduced affinity toward small ligands such as azide, thiocyanate, and H_2O_2. In fact, H_2O_2 is a poor substrate compared to many alkyl peroxides (44). The low affinity of azide and thiocyanate for COXs probably arises from unfavorable interactions with distal "roof" residues in the POX active site (Figure 5), but the crystal structures provide little insight into how this occurs.

The proximal His is bonded directly to an Asn in MPO (95) and to an Asp in cytochrome *c* peroxidase (61), creating a more basic proximal ligand. Such strong interactions on the proximal side of the heme are considered to control the reactivity of the heme iron. In ovine COX-1, resonance Raman spectroscopy indicates that His388, the proximal ligand, is clearly more neutral in character than the corresponding proximal ligands found in other peroxidases (68). Although His388 in COX-1 hydrogen bonds to Tyr504 via a mediating buried water, mutating Tyr504 to an alanine results in only a marginal loss in POX activity (68). Thus, the proximal His in COX requires no backside hydrogen bond to catalyze peroxidation. However, this difference in acidity of the proximal histidine in native COX is clearly not reflected in the rate of POX turnover, which is comparable to those of other heme peroxidases (78).

The relatively facile removal of heme for COX-1 and -2 has allowed the creation of apo-enzyme and its reconstitution into pseudo-holoforms of COX with different metallo-protoporphyrin IX compounds. Although Fe^{3+}-protoporphyrin IX is the natural heme ligand, Mn^{3+}-protoporphyrin IX can slowly undergo the changes in redox state needed for POX catalysis and can initiate the COX reaction (89, 90). Other metals (e.g., Zn or Co) in protoporphyrin IX do not support either the POX or COX reactions (52). However, ovine COX-1 reconstituted with Co^{3+}-protoporphyrin IX does form a native-like, albeit inactive, enzyme form with

the metal bound in a six-coordinate state (39). This form of the enzyme was useful for creating stable complexes of ovine COX-1 with fatty acid substrates for crystallographic analyses (38–40, 87).

THE COX ACTIVE SITE

The backbone folding in the interior of COX is homologous to that found in MPO, particularly in the region around *helix 6* through the turn and extended strand that follow it. In COX, however, this strand is shifted by ~7 Å from that seen in MPO (13). This structural alteration opens up the enzyme's interior to create the ~25 Å long COX channel (Figure 3*c*); such interior cavities are unknown in MPO and other related heme-dependent peroxidases. The COX catalytic center encompasses the upper half of a channel, extending from Arg120 to Tyr385. From an evolutionary perspective, an ancestral peroxidase must have undergone two distinct changes to create COX: (*a*) the formation of an interior channel for the COX reaction and (*b*) the acquisition of the membrane binding.

The mechanism of substrate interactions with COX-1 and -2 is becoming better understood with the growing number of COX structures containing bound substrates (22, 29, 38, 40, 87). In ovine COX-1, AA binds in an extended L-shaped but kinked conformation (Figure 3*c*). The guanidinium group of Arg120 ligands the carboxylate of the fatty acid; this interaction is a known determinant of substrate binding in COX-1 (2, 38, 64). Carbons 7 through 14 of AA form an S-shape that weaves the substrate chain around the side chain of Ser530, the residue acetylated by aspirin (8, 34). AA is positioned such that carbon 13 is oriented near the phenolic oxygen of Tyr385 (Figure 6), where the *proS* hydrogen can be abstracted to initiate the COX reaction. The ω-end of AA (carbons 14 through 20) binds in a hydrophobic groove above Ser530, where Phe205, Phe209, Val344, Phe381, and Leu534 stabilize its conformation.

The alternative fatty acid substrates DHLA (20:3n-6), LA (18:2n-6), and EPA (20:5n-3) also bind to the COX active site in extended L-shaped conformations (Figure 6*b*) that are generally similar to those observed for AA (40, 87). These alternative substrates have their carboxylate group positioned such that it makes the critical salt bridge with Arg120, and the ω-end is placed in the hydrophobic groove above Ser530. The alternative substrates make contact with virtually the same set of residues within the active site as AA. However, the chemical differences in polyunsaturation and carbon length presented by DHLA, EPA, and LA lead to local differences in the bound conformation compared to AA. The level of conformational flexibility in each fatty acid impacts the alignment (or misalignment) of the carbon targeted for hydrogen abstraction by Tyr385 (40, 87). For example, LA (18:2n-6) is two carbons shorter and contains two fewer double bonds than AA (20:4n-6). The Arg120/carboxylate interaction is maintained, and carbons 1 to 6 of LA are positioned similarly to the equivalent carbons in AA. However, carbons 7 through 9 display a more extended stereochemistry; this positions carbon 11, instead of carbon 13, below Tyr385 at the top of the active site (40). Thus, 9- or 13-hydroperoxy octadecadienoic acids can be produced. Other fatty acids such as

18:3n-6 and 20:2n-6 should bind in a similar manner that would permit removal of the n-8 hydrogen; 18:3n-3, however, would need to be aligned for abstraction of the n-5 hydrogen (31, 65).

The attempts to study the structure of AA in COX-2 (22, 29) have yielded interesting but somewhat more equivocal results that underscore the difficulty in obtaining crystals of COX complexes with such unstable substrates. Kiefer et al. (22) reported the structure of mouse COX-2 crystallized in the presence of AA. Although they used the apo-form of the enzyme to prevent the turnover of AA during crystallization, they observed a pattern of electron density that suggested a mixture of bound substrate (AA) and product (PGG_2). After building both molecules into the COX active site, Kiefer and colleagues (29) found an almost identical set of interactions between the protein and ligand as seen in COX-1. In another attempt to prevent turnover of the substrate during crystallization, Kiefer et al. (22) made an H270A mutation to create a POX inactive version of the enzyme. The pattern of electron density again suggested that ligand had bound, but in a substantially different conformation. After careful model building at 2.4 Å resolution, Kiefer and colleagues concluded (22, 29) that AA had bound in a nonproductive, "backward" conformation, i.e., with the carboxylate hydrogen-bonded to Tyr385 and Ser530. Kiefer and colleagues (22, 29) consider this second binding mode for AA as an inhibitory binding state in COX-2 and have recently shown that EPA binds to COX-2 in an equivalent fashion. The COX active site in COX-2 is larger than in COX-1 (28, 37) and may thus accommodate a wider array of alternative conformations for many ligands than is allowed in COX-1.

While the physiological relevance of this "inhibitory" binding mode is not clear, it does, however, highlight the markedly different behavior of COX-2 toward ligands compared with that of COX-1 despite a high degree of sequence and structural homology in this region. Several interesting facts have recently come to light that suggest that the conversion of alternate substrates by the COX enzymes to oxygenated products other than PGH_2 may have significant physiological relevance. For example, COX-2 seems to be able to convert the endocannabinoids 2-arachidonylglycerol and arachidonylethanolamide into the precursors for prostaglandin glycerol esters and prostaglandin ethanolamides (23, 24, 62). Understanding the physiological roles of these alternative prostaglandins may clarify the role of COX-2 in the central nervous system. Moreover, many of the minor products from the COX reactions with arachidonate and other fatty acids have significant biological activities (70). Thus, how alternative substrates are utilized differently by COX-1 and -2 may impact the therapeutic effects of diet and NSAID use on cancer, arthritis, and cardiovascular disease.

STRUCTURAL INSIGHTS FROM MUTAGENESIS

The structures of COX complexed with fatty acids (22, 38, 40, 87) have allowed more detailed interpretations of how mutagenesis of active site residues impacts the catalytic steps leading to PGG_2 formation. Interestingly, mutagenesis of COX

enzymes clearly revealed that the isoforms behave in distinctly different ways. One striking example is Arg120, which was identified as a potentially critical contributor to substrate binding via the fatty acid carboxylate (28, 37, 58). Indeed, the substitution of Arg120 with other residues can markedly decrease AA affinity by up to 1000-fold (2, 41). In sharp contrast, similar mutations in human COX-2 have little effect on K_m or V_{max} (64). These results suggest that the hydrophobic residues in the COX-2 COX channel must play a more significant role in substrate binding than in COX-1. How they compensate for the surprisingly diminished role of Arg120 in COX-2 remains unclear.

The several other residues within the COX active site, besides Arg120, have been studied by mutagenesis in both isozymes (40, 67, 85, 87). Three regions of the active site have been studied extensively: Val349 near the apical portion of AA; Ser530, Tyr348, and Trp387 near the central portion of AA; and Phe518, Leu531, and Gly533 near the ω-end of the substrate. Mutations at three of these sites (Val349, Ser530, and Gly533) (Figure 6) seem to reveal a great deal about the effects of substrate/enzyme interactions on catalysis.

When Val349 is mutated in ovine COX-1 and human COX-2, 11*R*-HPETE, not PGG_2, is the major COX product (86). The mutation of Val349 to other amino acids also has an impact on the formation of PGG_2 and 15*R/S*-HPETE by-products (67, 85). The replacement of Val349 with leucine in ovine COX-1 eliminates all 11-HPETE formations, but increases the formation of the 15*R/S*-HPETE by-products as an equimolar mixture (85). When Schneider et al. (67) replaced valine with isoleucine at residue 349 in COX-1 or -2, they observed a marked shift in product stereochemistry at carbon 15 toward the *R* stereoisomer for both PGG_2 and 15-HPETE. Thus, Val349 may play a subtle role in maintaining the proper stereochemistry of the substrate during oxygen addition at carbon 15.

Ser530 is the site of acetylation by aspirin (32, 34, 72) and makes an intimate interaction with AA at carbon 13 (38, 85). While not essential for catalysis, Ser530 may help optimally align the substrate with respect to the Tyr385 for hydrogen abstraction (38, 94) at carbon 13, as well as for subsequent oxygen addition at carbon 11 (Figure 6). When Ser530 in COX-1 is mutated to a threonine, the enzyme is active, but 15*R*-HPETE is formed almost exclusively instead of PGG_2 (85). However, the acetylation of Ser530 by aspirin in COX-1, which adds three nonhydrogen atoms completely to the serine, now blocks the binding of AA and completely inactivates the enzyme. When aspirin acetylates human COX-2, substrate turnover still occurs, but 15*R*-HPETE is produced (32, 42). The additional atoms at position 530 apparently perturb the AA conformation in COX-2 so that oxygen insertion at carbon 15, but not at carbon 11, is possible after hydrogen abstraction. As the COX active site in COX-2 is larger than in COX-1 (28, 37), COX-2 can obviously accommodate larger moieties at position 530 without inactivating. Interestingly, Schneider et al. (67) found that replacing Ser530 in COX-2 with threonine resulted in an almost complete shift in product stereochemistry at carbon 15 toward the *R* stereoisomer in PGG_2, as well. Hence, the amino acid side chain at position 530 may play a critical role in determining the stereochemistry of oxygen addition at carbon 15.

At the very end of the fatty acid binding pocket, Gly533 (Figure 6) abuts on the very last two carbons of AA in COX-1 (38). Intriguingly, the mutation of this residue in ovine COX-1 and human COX-2 markedly decreases substrate turnover (65, 72, 85). The superimposed structures of AA, DHLA, EPA, and LA (40, 87) clearly show that the ω-ends of the substrates tend to adopt a particular stereochemistry in this region of the active site (Figure 6*b*). Mutations at or near Gly533 must then perturb the conformation of the substrate away from the catalytically competent conformer (38, 65, 85). Thus, it seems that the positioning of the ω-end of a fatty acid substrate is a critical factor in its turnover (40, 87). If the tail of the substrate is not bound properly, then the appropriate hydrogen cannot be readily abstracted. On the other hand, the COX active site surrounding the carboxylate end of the fatty acids seems to better accommodate mutations without a major loss of COX activity (40, 87). This region of the active site may help compensate for any steric strain arising from the positioning of the substrate's ω-end for turnover.

THE COX REACTION REVISITED

The basic steps in the COX reaction, as originally proposed by Hamberg & Samuelsson (19), have remained virtually unchanged for over 30 years. The bulk of the biochemical and structural evidence supports all the central features of the Hamberg & Samuelsson mechanism (19, 29, 43, 45, 76), but recent structural studies have now highlighted some of the important structure-function relationships in PGG_2 formation. The COX reaction scheme can now be broken down into four basic steps (Figure 7). Initially, the arachidonyl carboxylate interacts with Arg120 (28, 34, 35, 37, 38, 58) and enters the COX channel. During this process, the enzyme appropriately positions the 13*proS* hydrogen of AA for abstraction. Carbons 8 through 12 are also positioned in a space suitable for the formation of the endoperoxide bridge and the cyclopentyl ring (38, 86). When AA is appropriately positioned, the rate-determining step begins: The radical on Tyr385 abstracts the 13-*proS* hydrogen. Subsequently, an 11*R*-peroxyl radical is quickly formed in the presence of oxygen. In the third step, the 11*R*-peroxyl radical attacks carbon 9 to form the endoperoxide, resulting in the isomerization of the radical to carbon 8. At this stage, ring closure between carbon 8 and carbon 12 cannot occur given the extended conformation exhibited by AA in the crystal structures (Figure 7). Therefore, a major reconfiguration of the substrate must occur concomitant with or immediately following formation of the endoperoxide bridge. This hypothetical conformational transition would involve a significant movement of the ω-end of the substrate toward the carboxyl half. The 11*R*-hydroperoxyl radical is hypothesized to swing "over" carbon 8 for an *R*-side attack on carbon 9 through the rotation about the carbon 10/carbon 11 bond, which brings carbon 12 closer to carbon 8 for the ring closure (Figure 7). This conformational transition would also reposition carbon 15 for the addition of the second molecule of oxygen. In the final step, the 15*S*-peroxyl radical is aligned below Tyr385 for donation of the radical to complete the catalytic cycle.

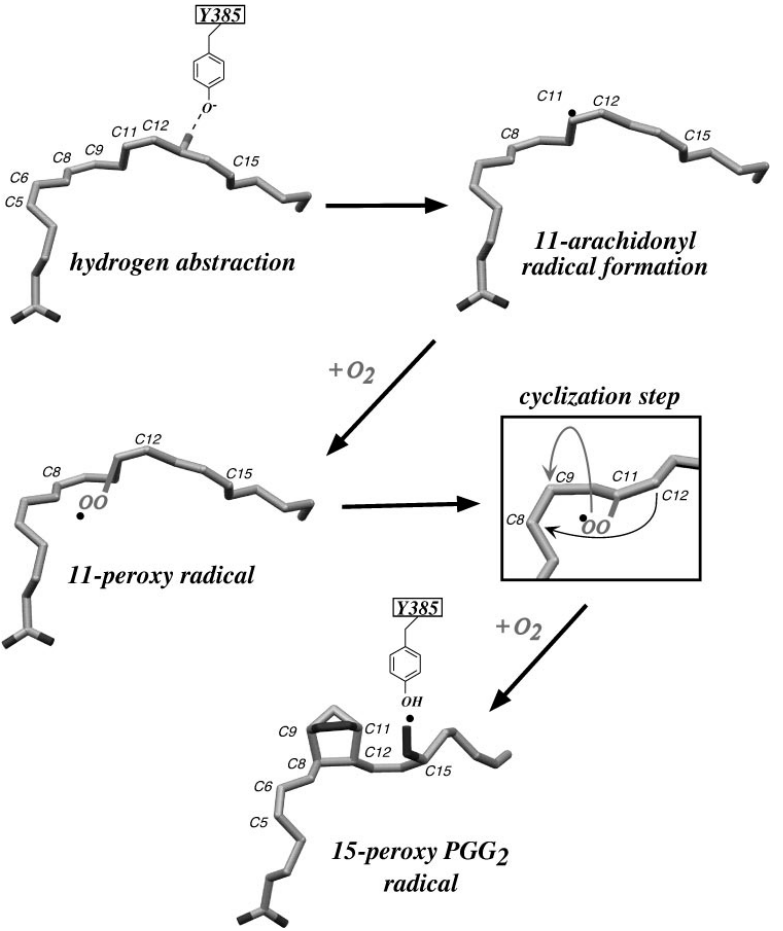

Figure 7 A schematic of the COX reaction as proposed by Malkowski et al. (38). While the formation of the 11-peroxy-arachidonate intermediate is explained by the crystal structure for the ovine COX-1/AA complex, its subsequent conversion to PGG_2 requires a major conformational transition that has not been observed or characterized.

While the formation of PGG_2 is now fairly well explained, why 11*R*-HPETE, 15*R*-HPETE, and 15*S*-HPETE are formed is unclear. Thuresson et al. (86) presented biochemical evidence that each COX product may arise from a different but catalytically competent conformer of AA. In essence, hydrogen abstraction can occur when AA is not in a conformation that allows facile ring closure, which then leads to the monooxygenation of the substrate. This may mean that the observed structure of AA bound in the COX-1 active site (38) may be a time- and space-average of more than one AA conformer, of which only the predominant conformer

leads to PGG_2 formation. As little conformational variation is seen in the COX-1 and -2 crystal structures, subtle but distinct dynamic transitions in enzyme structure must be occurring to account for the different substrate conformers in the native and mutant forms of COX. As mentioned earlier, the COX channel narrows considerably to form an aperture (Figure 3*c*). The aperture, composed of parts of the catalytic center and the MBD, must open and close during entry of fatty acid substrates and NSAIDs and egress of product (35). The subtle conformational dynamics of the COX active site and the MBD may be a primary factor in determining the final COX products. Interestingly, studies on enzyme inhibition by NSAIDs have provided strong evidence that conformational variation not observed in the crystal structures occurs in COX-1 and -2.

THE STRUCTURAL BASIS OF NSAID ACTION

Several detailed reviews have been recently published on this topic (7, 12, 50), and only a summary of the major highlights of NSAID inhibition in the COX isoforms is given here. NSAIDs are usually subdivided into two classes: (*a*) classical or "nonselective" NSAIDs and (*b*) COX-2-selective or "isoform-specific" NSAID inhibitors. The classical NSAIDs inhibit both COX-1 and -2, but many tend to bind more tightly to COX-1 (7, 50). In contrast, COX-2-selective inhibitors have been designed to exhibit significantly higher selectivity toward COX-2 than toward COX-1 (7, 50). While all NSAIDs compete with arachidonate for the COX active site, each NSAID can be classified by one of three general modes of action (7, 50). An NSAID can display (*a*) rapid, reversible competitive inhibition (e.g., ibuprofen), (*b*) rapid, reversible binding followed by covalent modification (e.g., the action of aspirin on Ser530), or (*c*) rapid, lower-affinity competitive inhibition followed by a time-dependent transition to a high-affinity slowly reversible inhibitory mode (e.g., flurbiprofen). The structural basis for time-dependent inhibition is not yet well defined and may be different for different drugs. Moreover, the kinetic differences in NSAID inhibition have made simple comparisons of drug interactions between COX-1 and COX-2 difficult.

Figure 8 illustrates the basic features of NSAID binding to COX-1 and -2. The drugs generally bind within the upper part of the COX channel between Arg120 and Tyr385. The acidic class of NSAIDs (e.g., profens and fenamates) interact with Arg120 in both COX isozymes (7, 12) via hydrogen bonding or electrostatic interactions that provide a major portion of the binding energy and selectivity. The remaining drug/protein interactions tend to be hydrophobic (7, 12) except for potential hydrogen bonding to Ser530.

The differences between classical NSAIDs and COX-2 inhibitors arise in part from slight differences in the amino acids surrounding the active sites of COX-1 and -2. Within the catalytic center, only one structural difference is seen: Ile523 in COX-1 is substituted with Val523 in COX-2. This minor and conservative change results in a small side pocket becoming more accessible from the active

site channel (28, 37). In the second shell of amino acids surrounding the COX active site, Ile434 in COX-1 is substituted by a valine in COX-2. Again, this minor substitution, coupled with the Val523, increases the accessible volume of the active site channel by enhancing the mobility of local side chains (28, 37). Hence, the combination of Val523 and Val434 in COX-2 allows a movement of Phe518 and permits access to the polar side pocket (Figure 8*b*). The larger main channel combined with this side pocket increases the volume of the COX-2 NSAID binding site by about 20% over that in COX-1 (28, 37). The larger effective size of the channel in the COX-2 may also preferentially reduce steric and ionic crowding by Arg120 in COX-2 and thus may enhance the binding of nonacidic NSAIDs to COX-2.

This extra volume is a structural feature exploited by most COX-2 inhibitors. Mutating Val523 to an isoleucine restricts access to this side pocket, and COX-2 is no longer differentially sensitive to these inhibitors (15, 18). Conversely, an I523V mutation in COX-1 increases its affinity for COX-2 inhibitors (93). The substitution of His513 in COX-1 with arginine in COX-2 also alters the chemical environment of the side pocket by placing a stable positive charge at its center (28). This arginine seemingly interacts with polar moieties entering the pocket. In combination with the I523V mutation, an H513R mutant of COX-1 becomes much more sensitive to COX-2 inhibitors (93).

TIME-DEPENDENT INHIBITION AND CONFORMATIONAL TRANSITIONS

COX is known to undergo significant conformational changes following binding of heme, fatty acid substrates, and NSAIDs (4, 26). The phenomenon of time-dependent inhibition also provides quite credible evidence of conformation changes in COXs (7, 76), where the enzymes shift from a freely reversible enzyme/ligand complex EI to a tight-binding, slowly reversible EI* complex. The fact that the new COX-2 inhibitors display time-dependent inhibition toward COX-2, but freely reversible inhibition toward COX-1, has provided a new and intriguing view of NSAID action (7, 15, 18). Mutagenesis experiments have suggested that time-dependent inhibition of COX-2 by isoform-selective inhibitors containing sulfonamide or methylsulfoxide moieties may arise from their interaction with Arg513 (28, 93). Curiously, the time-dependent inhibition displayed by the methylsulfoxide inhibitor NS-398, an early lead compound, appears to depend on interaction with Arg120 but not with Arg513. The R120E and R120Q mutations in COX-2 result in simple competitive inhibition by NS-398 (16, 64), suggesting that NS-398 binds in the COX-2 active site similarly to acidic inhibitors such as flurbiprofen.

Unfortunately, determining the precise physical basis for time-dependent inhibition has been elusive. The observed crystal structures of the COX isoforms have provided little insight into the phenomenon. In fact, the crystal structures

of COX-1 with time-dependent inhibitors or competitive inhibitors are essentially indistinguishable (69). In the one case where ligand binding in human COX-2 did perturb the MBD (37), the changes were relatively minor. Why do the COX isoforms exhibit a single major conformation in crystals, regardless of whether a COX ligand is bound or not? Adding to this dilemma is the fact that the narrow aperture within the COX channel (Figure 3*c*) effectively buries all bound ligands within the catalytic domain (35, 38). As all ligands must enter the COX active site through the MBD, the COX channel region must undergo significant conformational changes during substrate entry and product exit. Recent studies (80, 92) have suggested that the reorganization of hydrogen bonding networks within the MBD (80) may play an active role in substrate binding, catalytic efficiency, and inhibition by NSAIDs. One hypothesis is that at least two conformations of the enzyme exist in equilibrium (80): an unstable ligand-free form and a more stable ligand-bound form. Conformational models have been proposed to explain time-dependent inhibition (80, 92), but how these conformational transitions are controlled and impact substrate and NSAID binding are, as yet, unanswered.

Identifying the nature of the EI^* state associated with time-dependent inhibition might be easier. In the active COX, AA is rapidly converted to PGG_2 and then released. During this process, a conformational rearrangement of the AA chain must occur within the active site as the cyclopentane ring and endoperoxide bridge form (38). This structural transition may disrupt a hydrogen bond network within the COX channel and facilitate release of the newly formed product PGG_2. Thus, COX may shuttle between two conformational states as part of the catalytic mechanism for bis-oxygenation. Time-dependent inhibition may occur when NSAIDs trap the most stable conformation, i.e., that seen in the crystal structures, but then may not be able to trigger the conformational change needed for facile release. Thus, time-dependent inhibition may be a serendipitous outcome of a catalytic mechanism involving two distinct conformational steps (80, 92). Nonetheless, identification and characterization of the important conformational transitions in COX remain elusive, but these structural events will have a major impact on our understanding of how NSAIDs interact with COX. As the crystallographic research on COX continues to mature and as higher-resolution structures become available, we may be able to resolve these and the other remaining questions about the structure-function relationships in COX.

ACKNOWLEDGMENTS

NIH Grants R01 HL56773 and P01 GM57323 supported work from the author's laboratory that was mentioned in this review. The author is grateful to a number of colleagues for their personal communications regarding unpublished work on COX. The author would also like to thank Dr. Guenter Trummlitz and colleagues at Boehringer-Ingelheim for providing the raw image for Figure 3*c*.

The *Annual Review of Biophysics and Biomolecular Structure* is online at http://biophys.annualreviews.org

LITERATURE CITED

1. Barnett J, Chow J, Ives D, Chiou M, Mackenzie R, et al. 1994. Purification, characterization and selective inhibition of human prostaglandin G/H synthase 1 and 2 expressed in the baculovirus system. *Biochim. Biophys. Acta* 1209:130–39
2. Bhattacharyya DK, Lecomte M, Rieke C, Garavito RM, Smith WL. 1996. Involvement of arginine 120, glutamate 524, and tyrosine 355 in the binding of arachidonate and 2-phenylproprionic acid inhibitors to the cyclooxygenase active site of ovine prostaglandin endoperoxide H synthase-1. *J. Biol. Chem.* 271:2179–84
3. Campbell ID, Bork P. 1993. Epidermal growth factor-like modules. *Curr. Opin. Struct. Biol.* 3:385–92
4. Chen Y, Bienkowski M, Marnett L. 1987. Controlled tryptic digestion of prostaglandin H synthase. Characterization of protein fragments and enhanced rate of proteolysis of oxidatively inactivated enzyme. *J. Biol. Chem.* 262:16892–99
5. Crofford LJ, Lipsky PE, Brooks P, Abramson SB, Simon LS, van de Putte LB. 2000. Basic biology and clinical application of specific cyclooxygenase-2 inhibitors. *Arthritis Rheum.* 43:4–13
6. Davy C, Fenna R. 1996. 2.3 Å resolution X-ray crystal structure of the bisubstrate analogue inhibitor salicylhydroxamic acid bound to human myeloperoxidase: a model for a prereaction complex with hydroperoxide. *Biochemistry* 35:10967–73
7. DeWitt DL. 1999. COX-2 selective inhibitors: the new super aspirins. *Mol. Pharmacol.* 4:625–31
8. DeWitt DL, El-Harith A, Kraemer SA, Andrews MJ, Yao EF, et al. 1990. The aspirin and heme-binding sites of ovine and murine prostaglandin endoperoxide synthases. *J. Biol. Chem.* 265:5192–98
9. Dietz R, Nastainczyk W, Ruf H. 1988. Higher oxidation states of prostaglandin H synthase. Rapid electronic spectroscopy detected two spectral intermediates during the peroxidase reaction with prostaglandin G2. *Eur. J. Biochem.* 171:321–28
10. Evans SV. 1993. SETOR: hardware-lighted three-dimensional solid model representations of macromolecules. *J. Mol. Graphics* 11:134–38
11. Gajhede J, Schuller A, Henriksen A, Smith AT, Poulos TL. 1997. Crystal structure of horseradish peroxidase C at 2.15 Å resolution. *Nat. Struct. Biol.* 4:1032–38
12. Garavito RM, DeWitt DL. 1999. The cyclooxygenase isoforms: structural insights into the conversion of arachidonic acid to prostaglandins. *Biochim. Biophys. Acta* 1441:278–87
13. Garavito RM, Picot D, Loll PJ. 1994. Prostaglandin H synthase. *Curr. Opin. Struct. Biol.* 4:529–35
14. Gierse J, Hauser S, Creely D, Koboldt C, Rangwala SH, et al. 1995. Expression and selective inhibition of the constitutive and inducible forms of human cyclooxygenase. *Biochem. J.* 305:479–84
15. Gierse J, McDonald J, Hauser S, Rangwala S, Koboldt CM, Seibert K. 1996. A single amino acid difference between cyclooxygenase-1 (COX-1) and -2 (COX-2) reverses the selectivity of COX-2 inhibitors. *J. Biol. Chem.* 271:15810–14
16. Greig GM, Francis DA, Falgueyret JP, Ouellet M, Percival MD, et al. 1997. The interaction of arginine 106 of human prostaglandin G/H synthase-2 with

inhibitors is not a universal component of inhibition mediated by nonsteroidal anti-inflammatory drugs. *Mol. Pharmacol.* 52:829–38

17. Guo Q, Kulmacz RJ. 2000. Distinct influences of carboxyl terminal segment structure on function in the two isoforms of prostaglandin H synthase. *Arch. Biochem. Biophys.* 384:269–79
18. Guo Q, Wang LH, Ruan KH, Kulmacz RJ. 1996. Role of Val509 in time-dependent inhibition of human prostaglandin H synthase-2 cyclooxygenase activity by isoform-selective agents. *J. Biol. Chem.* 271:19134–39
19. Hamberg M, Samuelsson B. 1967. On the mechanism of biosynthesis of prostaglandins E-1 and F-1 alpha. *J. Biol. Chem.* 242:5336–43
20. Herschman H. 1996. Prostaglandin synthase 2. *Biochim. Biophys. Acta* 1299:125–40
21. Kalgutkar AS, Zhao Z. 2001. Discovery and design of selective cyclooxygenase-2 inhibitors as non-ulcerogenic, anti-inflammatory drugs with potential utility as anti-cancer agents. *Curr. Drug Targets* 2:79–106
22. Kiefer JR, Pawlitz JL, Moreland KT, Stegeman RA, Hood WF, et al. 2000. Structural insights into the stereochemistry of the cyclooxygenase reaction. *Nature* 405:97–101
23. Kozak KR, Crews BC, Ray JL, Tai HH, Morrow JD, et al. 2001. Metabolism of prostaglandin glycerol esters and prostaglandin ethanolamides in vitro and in vivo. *J. Biol. Chem.* 276:36993–98
24. Kozak KR, Rowlinson SW, Marnett LJ. 2000. Oxygenation of the endocannabinoid, 2-arachidonylglycerol, to glyceryl prostaglandins by cyclooxygenase-2. *J. Biol. Chem.* 275:33744–49
25. Kraulis PJ. 1991. MOLSCRIPT: a program to produce both detailed and schematic plots of protein structures. *J. Appl. Crystallogr.* 24:946–50
26. Kulmacz RJ, Lands WE. 1982. Protection of prostaglandin H synthase from trypsin upon binding of heme. *Biochem. Biophys. Res. Commun.* 104:758–64
27. Kulmacz RJ, Lands WEM. 1987. Cyclooxygenase: measurement, purification and properties. In *Prostaglandin and Related Substances: A Practical Approach*, ed. C Benedetto, RG McDonald-Gibson, S Nigan, TF Slater, pp. 209–27. Washington, DC: IRL Press
28. Kurumbail R, Stevens A, Gierse J, McDonald J, Stegeman RA, et al. 1996. Structural basis for selective inhibition of cyclooxygenase-2 by anti-inflammatory agents. *Nature* 384:644–48
29. Kurumbail RG, Kiefer JR, Marnett LJ. 2001. Cyclooxygenase enzyme: catalysis and inhibition. *Curr. Opin. Struct. Biol.* 11:752–60
30. Landino LM, Crews BC, Gierse JK, Hauser SC, Marnett LJ. 1997. Mutational analysis of the role of the distal histidine and glutamine residues of prostaglandin-endoperoxide synthase-2 in peroxidase catalysis, hydroperoxide reduction, and cyclooxygenase activation. *J. Biol. Chem.* 272:21565–74
31. Laneuville O, Breuer D, Xu N, Huang Z, Gage DA, et al. 1995. Fatty acid substrate specificities of human prostaglandin-endoperoxide H synthase-1 and -2. Formation of 12-hydroxy-(9Z, 13E/Z, 15Z)-octadecatrienoic acids from alpha-linolenic acid. *J. Biol. Chem.* 270:19330–36
32. Lecomte M, Laneuville O, Ji C, DeWitt DL, Smith WL. 1994. Acetylation of human prostaglandin endoperoxide synthase-2 (cyclooxygenase-2) by aspirin. *J. Biol. Chem.* 269:13207–15
33. Li Y, Smith T, Grabski S, DeWitt DL. 1998. The membrane association sequences of the prostaglandin endoperoxide synthases-1 and -2 isozymes. *J. Biol. Chem.* 273:29830–37
34. Loll P, Picot D, Garavito R. 1995. The structural basis of aspirin activity inferred from the crystal structure of inactivated

prostaglandin H_2 synthase. *Nat. Struct. Biol.* 2:637–43

35. Loll P, Picot D, Garavito R. 1996. The synthesis and use of iodinated non-steroidal antiinflammatory drug analogs as crystallographic probes of the prostaglandin H_2 synthase cyclooxygenase active site. *Biochemistry* 35:7330–40
36. Loll PJ, Sharkey CT, O'Connor SJ, Dooley CM, O'Brien E, et al. 2001. O-acetylsalicylhydroxamic acid, a novel acetylating inhibitor of prostaglandin H2 synthase: structural and functional characterization of enzyme-inhibitor interactions. *Mol. Pharmacol.* 60:1407–13
37. Luong C, Miller A, Barnett J, Chow J, Ramesha C, et al. 1996. Flexibility of the NSAID binding site in the structure of human cyclooxygenase-2. *Nat. Struct. Biol.* 3:927–33
38. Malkowski MG, Ginell S, Smith WL, Garavito RM. 2000. The x-ray structure of prostaglandin endoperoxide H synthase-1 complexed with arachidonic acid. *Science* 289:1933–37
39. Malkowski MG, Theisen MJ, Scharmen A, Garavito RM. 2000. The formation of stable fatty acid substrate complexes in prostaglandin H2 synthase-1. *Arch. Biochem. Biophys.* 380:39–45
40. Malkowski MG, Thuresson ED, Lakkides KM, Rieke CJ, Micielli R, et al. 2001. Structure of eicosapentaenoic and linoleic acids in the cyclooxygenase site of prostaglandin endoperoxide H synthase-1. *J. Biol. Chem.* 276:37547–55
41. Mancini J, Riendeau D, Falgueyret J, Vickers P, O'Neill G. 1995. Arginine 120 of prostaglandin G/H synthase-1 is required for the inhibition by non-steroidal anti-inflammatory drugs containing a carboxylic acid moiety. *J. Biol. Chem.* 270:29372–77
42. Mancini JA, O'Neill GP, Bayly C, Vickers PJ. 1994. Mutation of serine-516 in human prostaglandin G/H synthase-2 to methionine or aspirin acetylation of this residue stimulates 15-R-HETE synthesis. *FEBS Lett.* 342:33–37
43. Marnett LJ. 2000. Cyclooxygenase mechanisms. *Curr. Opin. Chem. Biol.* 4:545–52
44. Marnett LJ, Maddipati KR. 1991. Prostaglandin H synthase. In *Peroxidases in Chemistry and Biology*, ed. J Everse, KE Everse, MB Grisham, pp. 293–334. Boca Raton, FL: CRC
45. Marnett LJ, Rowlinson SW, Goodwin DC, Kalgutkar AS, Lanzo CA. 1999. Arachidonic acid oxygenation by COX-1 and COX-2. *J. Biol. Chem.* 274:22903–6
46. McGeer PL, McGeer EG. 1999. Inflammation of the brain in Alzheimer's disease: implications for therapy. *J. Leukoc. Biol.* 65:409–15
47. Merrit E, Murphy M. 1994. Raster3D version 2.0—a program for photorealistic molecular graphics. *Acta Crystallogr. D* 50:869–73
48. Moore BC, Simmons DL. 2000. COX-2 inhibition, apoptosis, and chemoprevention by nonsteroidal anti-inflammatory drugs. *Curr. Med. Chem.* 7:1131–44
49. Morita I, Schindler M, Regier MK, Otto JC, Itori T, et al. 1995. Different intracellular locations for prostaglandin endoperoxide H synthase-1 and -2. *J. Biol. Chem.* 270:10902–8
50. Munroe D, Lau C. 1995. Turning down the heat: new routes to inhibition of inflammatory signaling by prostaglandin H2 synthases. *Chem. Biol.* 2:343–50
51. Nina M, Berneche S, Roux B. 2000. Anchoring of a monotopic membrane protein: the binding of prostaglandin H2 synthase-1 to the surface of a phospholipid bilayer. *Eur. Biophys. J.* 29:439–54
52. Ogino N, Ohki S, Yamamoto S, Hayaishi O. 1978. Prostaglandin endoperoxide synthetases from bovine vesicular gland microsomes. *J. Biol. Chem.* 253:5061–68
53. Otto J, Dewitt D, Smith W. 1993. N-glycosylation of prostaglandin endoperoxide synthases-1 and -2 and their orientations in the endoplasmic reticulum. *J. Biol. Chem.* 268:18234–42

54. Otto J, Smith W. 1996. Photolabeling of prostaglandin endoperoxide H synthase-1 with 3-trifluoro-3-(m-[125I]iodophenyl) diazirine as a probe of membrane association and the cyclooxygenase active site. *J. Biol. Chem.* 271:9906–10
55. Patrignani P, Panara MR, Greco A, Fusco O, Natoli C, et al. 1994. Biochemical and pharmacological characterization of the cyclooxygenase activity of human blood prostaglandin endoperoxide synthases. *J. Pharmacol. Exp. Ther.* 271:1705–12
56. Patrono C. 1994. Aspirin as an antiplatelet drug. *N. Engl. J. Med.* 330:1287–94
57. Picot D, Garavito R. 1994. Prostaglandin H synthase: implications for membrane structure. *FEBS Lett.* 346:21–25
58. Picot D, Loll PJ, Garavito RM. 1994. The X-ray crystal structure of the membrane protein prostaglandin H_2 synthase-1. *Nature* 367:243–49
59. Poulos T, Edwards S, Wariishi H, Gold M. 1993. Crystallographic refinement of lignin peroxidase at 2 Å. *J. Biol. Chem.* 268:4429–40
60. Poulos T, Freer S, Alden R, Edwards S, Skogland U, et al. 1979. The crystal structure of cytochrome *c* peroxidase. *J. Biol. Chem.* 255:575–80
61. Poulos TL, Fenna RE. 1994. Peroxidases: structure, function and engineering. See Ref. 72a, pp. 163–99
62. Prusakiewicz J, Kingsley P, Kozak K, Marnett L. 2002. Selective oxygenation of N-arachidonylglycine by cyclooxygenase-2. *Biochem. Biophys. Res. Commun.* 296:612–17
63. Raz A. 2002. Is inhibition of cyclooxygenase required for the anti-tumorigenic effects of nonsteroidal, anti-inflammatory drugs (NSAIDs)? In vitro versus in vivo results and the relevance for the prevention and treatment of cancer. *Biochem. Pharmacol.* 63:343–47
64. Rieke CJ, Mulichak AM, Garavito RM, Smith WL. 1999. The role of arginine 120 of human prostaglandin endoperoxide H synthase-2 in the interaction with fatty acid substrates and inhibitors. *J. Biol. Chem.* 274:17109–14
65. Rowlinson SW, Crews BC, Lanzo CA, Marnett LJ. 1999. The binding of arachidonic acid in the cyclooxygenase active site of mouse prostaglandin endoperoxide synthase-2 (COX-2). *J. Biol. Chem.* 274:23305–10
66. Schelvis JPM, Seibold SA, Cerda JF, Garavito RM, Arakawa T, et al. 2000. Interaction of nitric oxide with prostaglandin endoperoxide H synthase: implications for Fe-His bond cleavage in heme proteins. *J. Phys. Chem. B* 104:10844–50
67. Schneider C, Boeglin WE, Prusakiewicz JJ, Scott W, Rowlinson SW, et al. 2002. Control of prostaglandin stereochemistry at the 15-carbon by cyclooxygenases-1 and -2: a critical role for Serine 530 and Valine 349. *J. Biol. Chem.* 277:478–85
68. Seibold SA, Cerda JF, Mulichak AM, Song I, Garavito RM, et al. 2000. Peroxidase activity in prostaglandin endoperoxide H synthase-1 occurs with a neutral histidine proximal heme ligand. *Biochemistry* 39:6616–24
69. Selinsky BS, Gupta K, Sharkey CT, Loll PJ. 2001. Structural analysis of NSAID binding by prostaglandin H2 synthase: time-dependent and time-independent inhibitors elicit identical enzyme conformations. *Biochemistry* 40:5172–80
70. Serhan CN, Clish CB, Brannon J, Colgan SP, Gronert K, et al. 2000. Anti-microinflammatory lipid signals generated from dietary N-3 fatty acids via cyclooxygenase-2 and transcellular processing: a novel mechanism for NSAID and N-3 PUFA therapeutic actions. *J. Physiol. Pharmacol.* 51:643–54
71. Shimokawa T, Smith WL. 1991. Essential histidines of prostaglandin endoperoxide synthase. His-309 is involved in heme binding. *J. Biol. Chem.* 266:6168–73
72. Shimokawa T, Smith WL. 1992. Prostaglandin endoperoxide synthase: the aspirin

acetylation region. *J. Biol. Chem.* 267: 12387–92

72a. Sigal H, Sigel A, eds. 1994. *Metal Ions in Biological Systems*. New York: Marcel Dekker

73. Smith T, Leipprandt J, DeWitt DL. 2000. Purification and characterization of the human recombinant histidine-tagged prostaglandin H endoperoxide synthases-1 and -2. *Arch. Biochem. Biophys.* 374:195–200

74. Smith W, Garavito R, DeWitt D. 1996. Prostaglandin endoperoxide H synthases (cyclooxygenses)-1 and -2. *J. Biol. Chem.* 271:33157–60

75. Smith WL, DeWitt DL. 1996. Prostaglandin endoperoxide synthases-1 and -2. In *In Advances in Immunology*, ed. FJ Dixon, pp. 167–215. San Diego: Academic

76. Smith WL, DeWitt DL, Garavito RM. 2000. Cyclooxygenases: structural, cellular, and molecular biology. *Annu. Rev. Biochem.* 69:145–82

77. Smith WL, Eling TE, Kulmacz RJ, Marnett LJ, Tsai A. 1992. Tyrosyl radicals and their role in hydroperoxide-dependent activation and inactivation of prostaglandin endoperoxide synthase. *Biochemistry* 31: 3–7

78. Smith WL, Marnett LJ. 1994. Prostaglandin endoperoxide synthases. See Ref. 72a, pp. 163–99

79. Smythies J. 1996. On the function of neuromelanin. *Proc. R. Soc. London Ser. B* 263:487–89

80. So OY, Scarafia LE, Mak AY, Callan OH, Swinney DC. 1998. The dynamics of prostaglandin H synthases. Studies with prostaglandin H synthase-2 Y355F unmask mechanisms of time-dependent inhibition and allosteric activation. *J. Biol. Chem.* 273:5801–7

81. Song I, Smith WL. 1996. C-terminal Ser/Pro-Thr-Glu-Leu tetrapeptides of prostaglandin endoperoxide H synthases-1 and -2 target the enzymes to the endoplasmic reticulum. *Arch. Biochem. Biophys.* 334: 67–72

82. Song X, Lin HP, Johnson AJ, Tseng PH, Yang YT, et al. 2002. Cyclooxygenase-2, player or spectator in cyclooxygenase-2 inhibitor-induced apoptosis in prostate cancer cells. *J. Natl. Cancer Inst.* 94:585–91

83. Spencer AG, Thuresson E, Otto JC, Song I, Smith T, et al. 1999. The membrane binding domains of prostaglandin endoperoxide H synthases 1 and 2. Peptide mapping and mutational analysis. *J. Biol. Chem.* 274:32936–42

84. Thomas T, Nadackal TG, Thomas K. 2001. Aspirin and non-steroidal anti-inflammatory drugs inhibit amyloid-beta aggregation. *NeuroReport* 12:3263–67

85. Thuresson ED, Lakkides KM, Rieke CJ, Sun Y, Wingerd BA, et al. 2001. Prostaglandin endoperoxide H synthase-1: the functions of cyclooxygenase active site residues in the binding, positioning, and oxygenation of arachidonic acid. *J. Biol. Chem.* 276:10347–57

86. Thuresson ED, Lakkides KM, Smith WL. 2000. Different catalytically competent arrangements of arachidonic acid within the cyclooxygenase active site of prostaglandin endoperoxide H synthase-1 lead to the formation of different oxygenated products. *J. Biol. Chem.* 275:8501–7

87. Thuresson ED, Malkowski MG, Lakkides KM, Rieke CJ, Mulichak AM, et al. 2001. Mutational and X-ray crystallographic analysis of the interaction of dihomo-γ-linolenic acid with prostaglandin endoperoxide H synthases. *J. Biol. Chem.* 276:10358–65

88. Tsai A, Kulmacz RJ. 2000. Tyrosyl radicals in prostaglandin H synthase-1 and -2. *Prostaglandins Other Lipid Mediat.* 62: 231–54

89. Tsai A, Palmer G, Xiao G, Swinney DC, Kulmacz RJ. 1998. Structural characterization of arachidonyl radicals formed by prostaglandin H synthase-2 and

prostaglandin H synthase-1 reconstituted with mangano protoporphyrin IX. *J. Biol. Chem.* 273:3888–94

90. Tsai A, Wei C, Baek HK, Kulmacz RJ, Van Wart HE. 1997. Comparison of peroxidase reaction mechanisms of prostaglandin H synthase-1 containing heme and mangano protoporphyrin IX. *J. Biol. Chem.* 272:8885–94
91. van der Ouderaa FJ, Buytenhek M, Nugteren DH, Van Dorp DA. 1977. Purification and characterization of prostaglandin endoperoxide synthase from sheep vesicular glands. *Biochim. Biophys. Acta* 487:315–31
92. Walker MC, Kurumbail RG, Kiefer JR, Moreland KT, Koboldt CM, et al. 2001. A three-step kinetic mechanism for selective inhibition of cyclo-oxygenase-2 by diarylheterocyclic inhibitors. *Biochem. J.* 357:709–18
93. Wong E, Bayly C, Waterman HL, Riendeau D, Mancini JA. 1997. Conversion of prostaglandin G/H synthase-1 into an enzyme sensitive to PGHS-2-selective inhibitors by a double His513 → Arg and Ile523 → Val mutation. *J. Biol. Chem.* 272:9280–86
94. Xiao G, Tsai AL, Palmer G, Boyar WC, Marshall PJ, et al. 1997. Analysis of hydroperoxide-induced tyrosyl radicals and lipoxygenase activity in aspirin-treated human prostaglandin H synthase-2. *Biochemistry* 36:1836–45
95. Zeng J, Fenna RE. 1992. X-ray crystal structure of canine myeloperoxidase at 3 Å resolution. *J. Mol. Biol.* 226:185–207

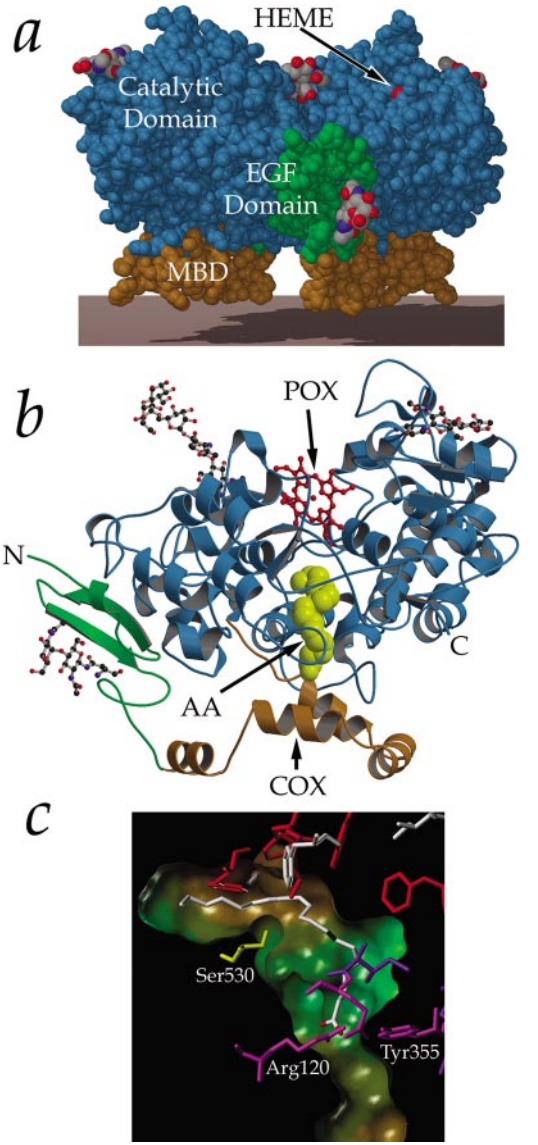

Figure 3 Structural representations of the ovine COX-1 dimer and monomer. (*a*) A space-filling view of the COX-1 dimer is shown. The EGF, MBD, and catalytic domains are colored green, gold, and blue, respectively. The locations of the heme in the POX active site are also shown, and the sites of N-linked glycosylation at asparagines N68, N144, and N410 appear as gray atoms. (*b*) A ribbon drawing shows the COX-1 monomer with bound arachidonic acid (AA in yellow) in the COX active site. The color scheme for the domains is the same as in (*a*). (*c*) A view of the COX channel with bound AA shows the aperture at the level of Tyr355 and Arg120. Views (*a*) and (*b*) were made with Molscript (25) and Raster3D (47).

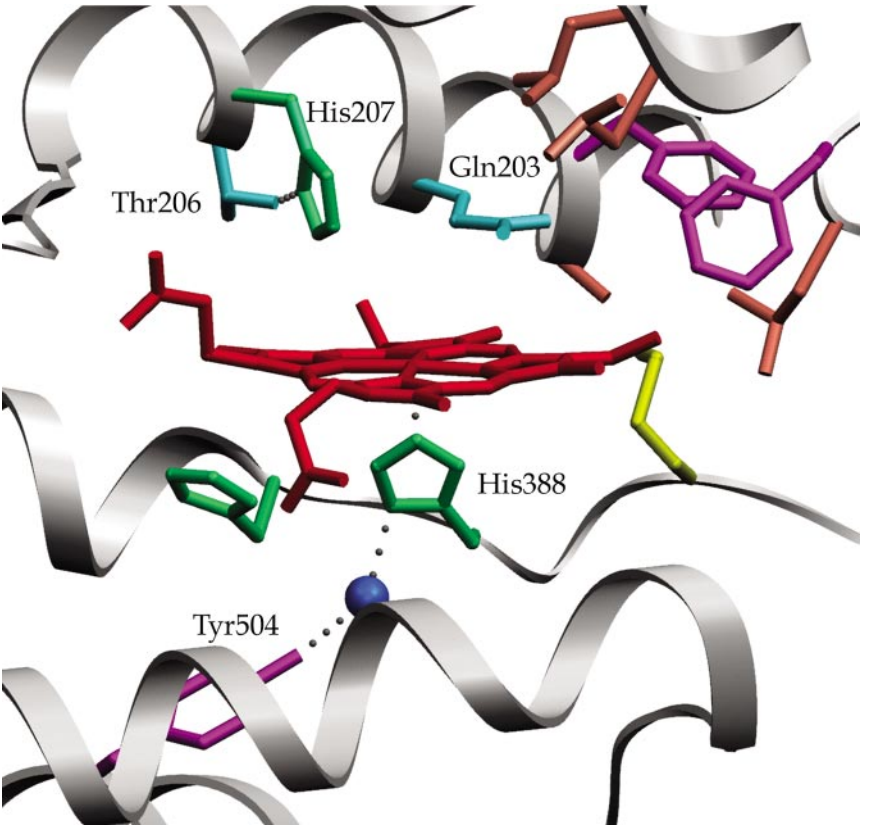

Figure 5 A view of the POX active site. The heme (red) is shown liganded to the proximal ligand His388 (green), which is hydrogen-bonded to a water molecule (blue) and Tyr504 (magenta). The distal residues His207 (green) and Gln203 (blue) are also shown. The nonpolar portion of some peroxide substrates may interact with the distal hydrophobic "roof" made up of valines and leucines (brown) and phenylalanines (magenta). Setor (10) was used to draw this figure and Figures 6 and 8.

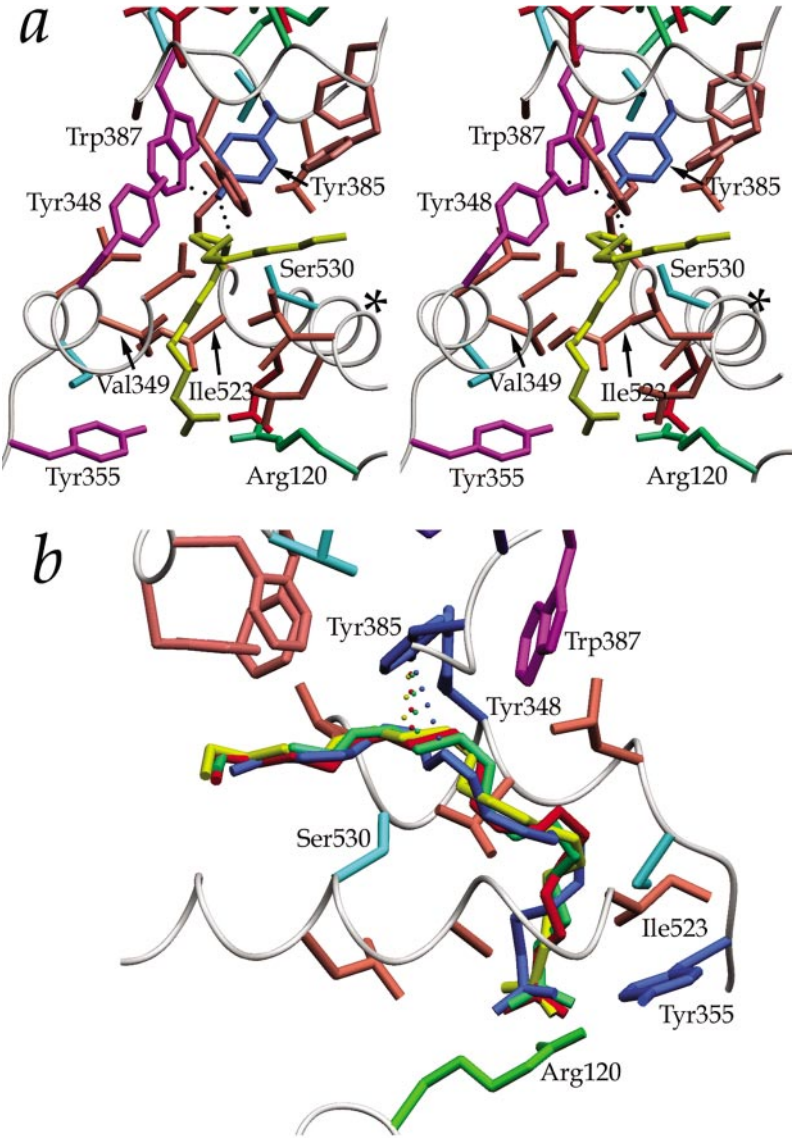

Figure 6 Fatty acid binding in ovine COX-1. (*a*) A stereo diagram of the COX active site shows the kinked L-conformation of AA (yellow). Note how Tyr385 (blue) is aligned with carbon 13 in AA, and how the carboxylate of arachidonate interacts with Arg120 (see text). Several other residues discussed in the text are also shown; the asterisk (*) refers to the position of Gly533. (*b*) A superposition of the fatty acids AA, DHLA (20:3n-6), LA (18:2n-6), and EPA (20:5n-3) in yellow, red, green, and blue, respectively, allows the comparison of their binding conformations in ovine COX-1. Note how the carboxylate ends of the fatty acids exhibit markedly different conformations, while the ω-ends adopt almost the equivalent conformations.

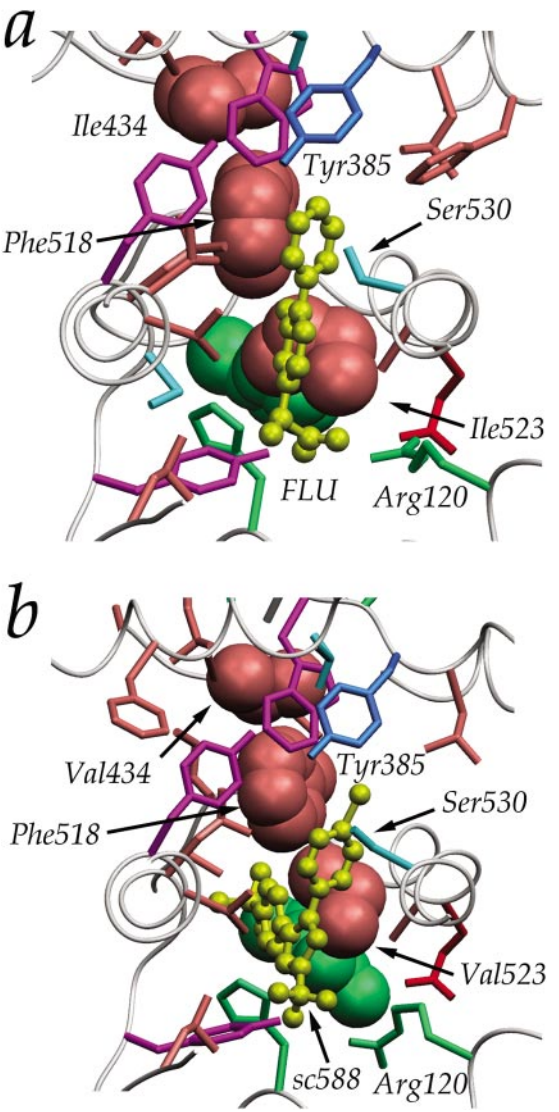

Figure 8 A view of NSAID binding in the COX active site. (a) Flurbiprofen (yellow) is bound in the COX active site channel in ovine COX-1 (58). Residues Ile 434 (copper), His513 (green), Phe518 (copper), and Ile523 (copper) are displayed as space-filling. (*b*) The COX-2 inhibitor SC-588 (yellow) is bound in the COX active site channel of mouse COX-2 (28). Residues Val434 (copper), Arg513 (green), Phe518 (copper), and Val523 (copper) are displayed as space-filling. The phenylsulfonamide group of SC-588 extends back into the side pocket made accessible by Val523 and interacts with Arg513. Access to the side pocket is made easier by the I434V change in COX-2, which then allows Phe518 to move out of the way when COX-2 inhibitors bind in this pocket.

Annual Review of Biophysics and Biomolecular Structure
Volume 32, 2003

CONTENTS